

Supplementary Methods

Cell culture

For transfections, *Drosophila* S2 cells were cultured in *Drosophila* SFM medium (GIBCO, Eggenstein, Germany), in a 40-ml culture flask in a 25°C incubator with 0.8% CO₂. L-glutamine-penicillin-streptomycin solution (GIBCO) was added to the medium prior to use (final concentrations 0.292 µg/ml, 1 unit/ml, 1µg/ml, respectively). 2.5 µg plasmid DNA or double stranded RNA in 200 µl antibiotic-free SFM containing 15 µl Cellfectin Reagent (Invitrogen, Carlsbad, CA) per 10⁶ cells were used. Copper sulfate (500 µM) was added to the medium 16 hours later to induce gene expression. 48 hours after transfection, cells were fixed for 10 minutes in 4% formaldehyde, 0.06 M NaPIPES, 0.03 M NaHEPES, 0.01 M NaEGTA, 4 mM MgSO₄, pH 6.8, permeabilized in PBS plus 0.5% saponin for 1 hour, and blocked by 2% donkey serum for 1 hour. Antibody and LysoTracker stains were used essentially as for larval staining. For trypsin digestion, transfected S2 cells were treated with 0.5% trypsin 0.2% EDTA solution (GIBCO) for 10-15 minutes, and centrifuged at 5000 rpm (EBA 12, Sartorius, Goettingen, Germany) for 5 minutes. The cell pellet was then resuspended in SFM and cells were allowed to settle on the bottom of the culture dish for 30 minutes. A GFP-gpi fragment¹ was used for expression in S2 cells (a gift from S. Eaton).

For quantification of fluorescence intensity in Supplementary Fig. 2, a transecting line was drawn on individual transfected cells using ImageJ (<http://rsb.info.nih.gov/ij/>). The percentage of total fluorescence within 0.5 µm of the plasma membrane on this line was calculated, and any cell for which this value was more than 30% was defined as showing redistribution of fluorescence to the plasma membrane. This was repeated for 50-70 cells from each of 10 fields of view in a single transfection, and an average number of cells showing redistribution was

obtained. Each transfection was repeated 5 times to allow statistical analysis. To quantify changes of Wit fluorescence intensity on the cell surface in Supplementary Fig. 5e, a transecting line was drawn on individual transfected cells using ImageJ. The percentage of total fluorescence within 0.5 μm of the plasma membrane on this line was calculated. This was repeated for 10-20 cells from two independent transfections to allow statistical analysis. A Mann-Whitney *U*-test was used for all statistical comparisons of S2 phenotypes. There was no significant difference between different transfections of the same construct.

Immunoprecipitation and immunoblot

For immunoprecipitation, crude serum was purified using Protein A beads, and purified antibodies were immobilized on AminoLink® Plus Coupling Gel (Pierce, Rockford, IL). Adult flies (1 ml) were collected in 1.5-ml microfuge tubes, frozen in liquid nitrogen, and homogenized in PBS containing 1% Triton X-100, 200 mM Ca^{2+} , 1.5 mM Mg^{2+} , and Protease Inhibitor Cocktail (Sigma, Poole, UK) for 30 minutes at room temperature. After centrifugation at 23,000g for 30 minutes, soluble proteins in the clear middle phase were diluted in PBS containing 0.2% Triton X-100. Diluted proteins were then preadsorbed on Protein A beads for 10 minutes, and filtered using a 0.2 μm filter (Sartorius, Goettingen, Germany). For immunoprecipitation, all procedures and reagents were from Pierce Seize Primary Immunoprecipitation Kit (Pierce, Rockford, IL). Fly extracts (Input) were incubated with immobilized antibodies for more than 2 hours at room temperature and the immune complex formed. The bound antigens were then eluted from the antibodies and collected (IP). *Drosophila* S2 cells were harvested and lysed in PBS containing 1% Triton X-100 and Protease Inhibitor Cocktail (Sigma, Poole, UK), and incubated at 4°C for 2 hours with anti-HA conjugated with agarose (Abcam, Cambridge, UK). The bound antigens (IP) were then washed 10 times with PBS containing 1% Triton X-100. For

western blot, immunoprecipitated material (IP), or fly extracts and S2 cell lysates prior to immunoprecipitation (Input) were resolved on a 12% SDS-PAGE gel. The gels were electroblotted onto nitrocellulose membranes, blocked with 5% nonfat dry milk in PBS for more than two hours, and incubated with primary antibodies.

Statistical analysis

Synaptic bouton numbers, NMJ length and branch numbers for each genotype were quantified at muscles 6/7 from segment A3, blind to genotype, using anti-synaptotagmin. All measurements were normalized relative to the surface areas of muscle 6 and 7. Cross-sectional areas of individual synaptic boutons were averaged for about 50-70 boutons per NMJ, and the values for individual NMJs were averaged across 10 larvae for each genotype. Any bouton with a cross-sectional area more than $3 \mu\text{m}^2$ was defined as type Ib and any bouton with a cross-sectional area less than $3 \mu\text{m}^2$ was defined as type Is; this criterion divided bouton size approximately into two unimodal distributions (data not shown). The percentage of type Ib boutons at the muscle 6/7 NMJ synapse accounted for $35.0 \pm 0.8\%$ in *spict^{mut}* and $36.5 \pm 0.7\%$ in *spict⁺* ($P = 0.14$, $n=10$). Proportions of Futsch-negative boutons for each genotype were quantified at muscles 6/7 from segment A3, blind to genotype, using anti-Futsch and anti-HRP. The average number of detectable Syt puncta was quantified in 100- μm lengths of segmental nerves passing through segment A4, or in segmental nerves passing through each segment, blind to genotype. The average number of axons per larva with Syt accumulations (an axon with Syt accumulations was defined as an axon in which more than 10 detectable Syt puncta were found) was quantified, blind to genotype.

For fluorescence intensity analysis, control and mutant larvae were dissected, stained and viewed in the same experiment under identical conditions. All larvae were stained and washed in

the same tube, with control larvae mouth-clipped or tail-clipped to allow them to be recognized after analysis. The intensities of control channel labelings in Fig. 3e-h, Fig. 4b or Supplementary Fig. 4d were calculated using ImageJ at one type Ib bouton at muscle 6/7 NMJ of segment A3, or at 200- μ m lengths of segmental nerves passing through segment A4, and defined as 1. The ratio of PMad, Tkv-HA or different tubulin marker intensities to control channel intensity was calculated for each individual larva. A Mann-Whitney *U*-test was used for all statistical comparisons of NMJ and axon phenotypes, except where otherwise indicated.

Wing size was calculated approximately as an ellipse, using the maximum length and width of at least 10 wings from 10 female flies, or from unsexed pupae. Body size was calculated approximately as the product of maximal lengths of sagittal, frontal and longitudinal axis of the body trunk, from 10 female flies.

Through the paper, distribution of data points is expressed as mean \pm standard error of the mean. Error bars represent standard error of the mean.

Reference

1. Greco, V., Hannus, M. & Eaton, S. Argosomes: A Potential Vehicle for the Spread of Morphogens through Epithelia. *Cell* **106**, 633-645 (2001).

Supplementary Figure 1. Localization of tagged Spict.

(a) S2 cells expressing a Spict-EGFP fusion stained for other endosomal and lysosomal markers.

(b) Localization of Spict-mRFP (expressed using *Actin5C-GAL4* in a *spict^{mut}* background), Spinster, and LysoTracker staining, at muscles 6 and 7 of segment A2 of 3rd instar larvae. The broken line shows the approximate boundary between muscles 6 and 7, along which the NMJ lies. All panels are single confocal sections. Scale bars: (a), 5 μm ; (b), 10 μm .

Supplementary Figure 2. Topology of Spict in S2 cells.

This result is consistent with either of the previous suggestions that Spict family members might have nine transmembrane domains¹, or be divergent members of the 7-TM superfamily².

(a) We first tested whether Spict-EGFP or EGFP-Spict, expressed in S2 cells, could be redistributed to the plasma membrane by blockage of endocytosis. Treatment with RNAi against *clathrin heavy chain* (*Chc*) caused redistribution of the Spict fusions towards the plasma membrane. A Spict-EGFP expression vector was used to transfect S2 cells, along with different RNA molecules. Cells treated with double stranded *Chc* RNA, but not those treated with control RNA (*pTRI-Xef1*), redistributed Spict-EGFP to the plasma membrane. The left two panels show projections of confocal sections of typical cells; the right panel shows quantification of cells that had at least 30% of Spict-EGFP fluorescence within 0.5 μm of the cell surface. Scale bar, 5 μm .

(b) Fluorescence of EGFP-Spict, but not of Spict-EGFP, is susceptible to exogenously added trypsin. Double stranded *Chc* RNA, together with expression vectors for Spict-EGFP, EGFP-Spict or GFP-gpi, were used to transfect S2 cells, which are subsequently treated with trypsin. Trypsin treatment significantly reduced the number of cells with EGFP-Spict and GFP-gpi at the cell surface; in the case of Spict-EGFP, it had no significant effect ($P = 0.5$). This suggested that *clathrin* RNAi treatment redistributed the fusion proteins to the cell surface, and that the N-

terminus of Spict is extracellular or luminal, and its C-terminus cytosolic. All panels show projections of confocal sections. For all comparisons with controls, *, $P < 0.05$; **, $P < 0.01$; ***, $P < 0.001$. n=5 transfections. Scale bars, 5 μm .

References

1. Chai, J.H., Locke, D.P., Grealley, J.M., Knoll, J.H., Ohta, T., Dunai, J., Yavor, A., Eichler, E.E. & Nicholls, R.D. Identification of four highly conserved genes between breakpoint hotspots BP1 and BP2 of the Prader-Willi/Angelman Syndromes deletion region that have undergone evolutionary transposition mediated by flanking duplicons. *Am J Hum Genet.* **73**, 898-925 (2003).
2. Lefèvre, [C.](#), Bouadjar, B., Karaduman, A., Jobard, F., Saker, S., Ozguc, M., Lathrop, M., Prud'homme, J.F. & Fischer, J. Mutations in ichthyin a new gene on chromosome 5q33 in a new form of autosomal recessive congenital ichthyosis. *Hum. Mol. Gen.* **13**, 2473-2482 (2004).

Supplementary Figure 3. *spict* null mutants cause synaptic overgrowth at the NMJ.

Quantification of normalized length (a) and branch numbers (b) of NMJs of muscle 6/7 of hemisegment A3, for each genotype shown in Fig. 3b. *spictR* represents *spict-mRFP*.

(c) NMJ overgrowth (shown by anti-synaptotagmin) in segments A4-5 in *spict^{mut}* third instar larvae. Anterior is on the top and midlines are indicated by near-vertical lines in the middle of each panel. Muscles are numbered. Synaptic boutons are stained by anti-synaptotagmin. Scale bar, 50 μm .

(d) NMJ overgrowth at muscle 6/7 of A6 in a *spict^{mut}* larva. Scale bar, 50 μm .

(e) Quantification of normalized bouton numbers in each genotype shown in d and in rescue

genotypes.

Panels in **c** and **d** are projections of confocal sections. For comparisons with *spict*⁺: *, $P < 0.05$; **, $P < 0.01$; ***, $P < 0.001$. n=20 larvae.

Supplementary Figure 4. BMP signaling is required for synaptic overgrowth in *spict*^{mut}, and for microtubule stability and axonal transport.

(a) Projections of confocal sections, showing synaptic boutons (visualized with anti-synaptotagmin) at muscles 6/7, hemisegment A3 of wild type (+) or *spict*^{mut} third instar larvae. Homozygous (top 4 rows) or heterozygous (bottom 4 rows) mutations in *med*, *sax*, *tkv*, and *wit* suppress the NMJ overgrowth (Fig. 3c-d) seen in *spict*^{mut} larvae. Please refer to Methods for exact genotypes. Scale bar, 50 μm .

(b,i) PMad staining of cell body nuclei in the ventral nerve cord (examples inside broken lines) in *spict*⁺, and an increase of nuclear PMad intensity in *spict*^{mut} cell bodies, which can be rescued (*spict*^{rescue}) by neuronal expression of *UAS-spict* using *elav-GAL4* in a *spict*^{mut} background. Nuclear PMad intensity is significantly decreased in *tkv* (*tkv*⁷/*tkv*¹⁶⁷¹³) cell bodies, and by overexpression of Spict by either pan-neuronal *elav-GAL4* or motoneuron-specific *OK6-GAL4*. Scale bar, 5 μm . (ii) Quantification of the intensity of PMad staining within the ventral nerve cord for each genotype shown in *i*. All comparisons are with *spict*⁺ (left bar). * $P < 0.05$, n=4 larvae.

(c) Single confocal sections show that levels of neuronal membrane proteins Fasciclin II, Syntaxin, and the anti-horseradish peroxidase antigen (HRP), are not obviously changed at *spict*^{mut} NMJs (mean intensity $P = 0.2$, 0.4 and 0.2 respectively, compared to *spict*⁺, n=5 larvae). Scale bar, 5 μm .

(d) Quantification of the intensity of α -tubulin (*i*) or acetylated- α -tubulin (*ii*) in presynaptic

boutons. Fluorescence intensity per voxel is normalized to a control channel (anti-HRP). The mean intensity of anti-HRP is not significantly different among the eight genotypes in each panel ($P > 0.68$, $n=6$ larvae, one-way ANOVA), and is assigned as 1 for each genotype. All comparisons are with w^{1118} (left bar) unless indicated. *, $P < 0.05$; **, $P < 0.01$, $n=6$ larvae.

(e) Quantification of boutons with Futsch-negative staining in genotypes shown in Fig. 4c,ii. The proportion of Futsch-negative boutons is increased in tkv^7/tkv^{16713} or $OK6-GAL4 UAS-spict$ compared to $OK6-GAL4$ ($P = 0.000$ or 0.001 respectively, $n=8$ larvae). Expression of $UAS-Act-Tkv$ reduces the proportion of Futsch-negative boutons in $OK6-GAL4 UAS-spict$ to wild-type levels ($P = 0.105$ compared to $OK6-GAL4$, $n=8$ larvae).

(f) Quantification of average number of segmental nerves per larva in which Syt accumulations were found. $OK6-GAL4 UAS-spict$ or tkv (tkv^7/tkv^{16713}) caused a significant increase ($P < 0.001$, $n=10$ larvae) in the numbers of affected nerves per larva compared to $OK6-GAL4$. tkv^{rescue} ($tkv^7 OK6-GAL4/tkv^{16713}$; $UAS-tkv-HA$) rescues the phenotype ($P = 1$ compared to $OK6-GAL4$). The presence of $tkv/+$ significantly increased, and expression of $UAS-Act-Tkv$ significantly decreased ($P < 0.001$, $n=10$, comparisons to $OK6-GAL4 UAS-spict$) the number of $OK6-GAL4 UAS-spict$ axons that were affected, but had no effect on axons that did not express $UAS-spict$.

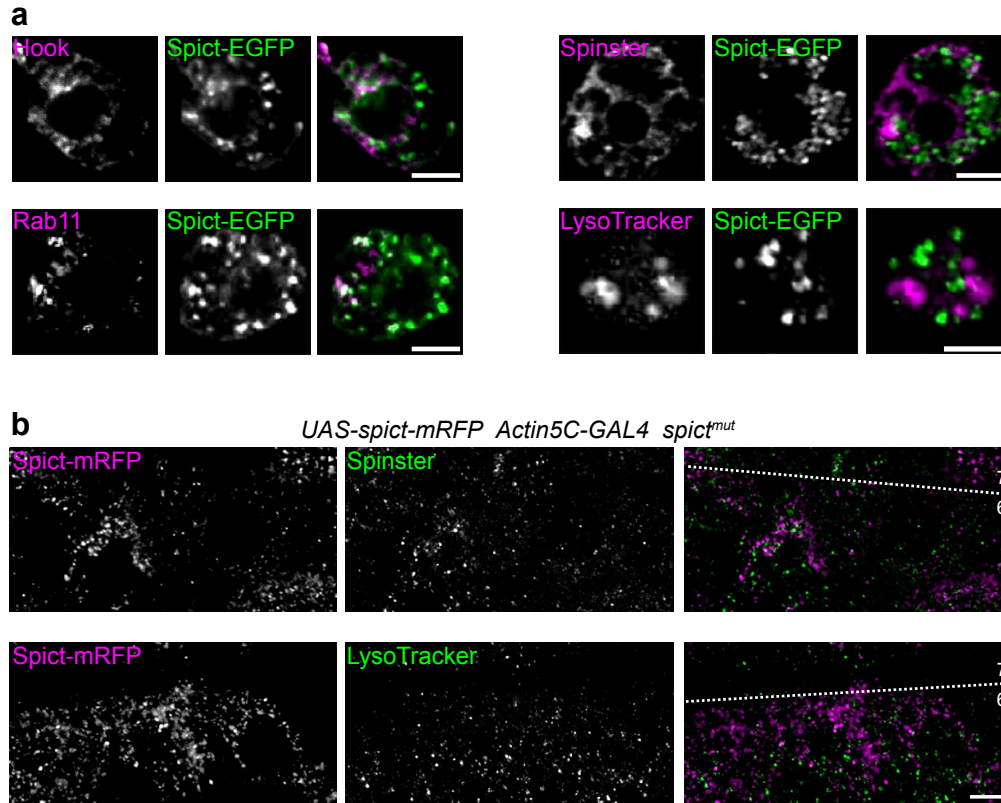
(g) The number of Syt puncta per segment per nerve, in segmental nerves passing through each segment from A1 to A6, showed no correlation with the position of the segments; linear fit, $r = -0.016$, $P = 0.906$, $n=10$ larvae.

Supplementary Figure 5. Involvement of Spict in BMP signaling.

(a-b) Spict and BMP signaling markers. (a) Western blot of larvae of genotypes wit^+ (w^{1118}) and wit^{A12} using antibody against Wit, and antibody against β -tubulin as a loading control. Note the level of total tubulin is not obviously decreased in wit^{A12} larval extract. (b) Whole blots of input

extracts shown in Fig. 7a. Arrows indicate the bands shown in Fig. 7a. (c) Western blot of larvae of *spict*⁺ and *spict*^{mut} was probed with anti-Wit and anti- β -tubulin as a loading control. The same amount of larval extract was loaded in each lane. Note that the levels of both Wit and total tubulin are not obviously changed in *spict*^{mut} larval extract. (d) A Western blot of cell lysate untreated (wild type, *wt*) or treated with *spict* RNAi (*spict* RNAi) was probed with anti-Spict. The same amount of cell lysate was loaded in each lane. (e) The intensity of Wit within 0.5 μ m of the cell surface was significantly increased in *spict* RNAi-treated cells, and significantly decreased in Spict-EGFP-transfected cells ($P < 0.001$, $n=10-20$ cells from 2 transfections). (f) S2 cells were transfected with *UAS-wit* and *Actin5C-GAL4* (*i-iii*, all rows), and *pMT-spict-EGFP* (*i-iii*, bottom rows). Late endosomes are labeled by anti-Hook, recycling endosomes by anti-Rab11, and late endosomes/lysosomes by anti-Spinster. In S2 cells without Spict-EGFP cotransfection (*i-iii*, top rows), Wit is predominantly localized to the cell surface, and shows no substantial overlap with the intracellular compartment markers. In S2 cells cotransfected with Spict-EGFP (*i-iii*, bottom rows; also see Fig. 7f), Wit overlaps with Spict-EGFP substantially in early endosomes (Rab5; Fig. 7f), but little in late endosomes (Hook; *i*), or recycling endosomes (Rab11; *ii*), or late endosome/lysosomes (Spinster; *iii*). Examples of triple colocalization are shown with arrows; note the greater extent of colocalization of Spict-EGFP and Wit with Rab5 than with Hook, Rab11 or Spinster (compare Fig. 7f and this figure). Panels are single confocal sections. Approximate cell boundaries are indicated by broken lines. Scale bars, 5 μ m. (g) Projections of confocal sections of pupal wing imaginal discs (30 hours after pupariation, upper row) and embryos (stage 6, bottom row), showing PMad expression. L4, L5, longitudinal vein 4, 5; PCV, posterior crossvein. Scale bars, 100 μ m.

Supplementary Figure 1

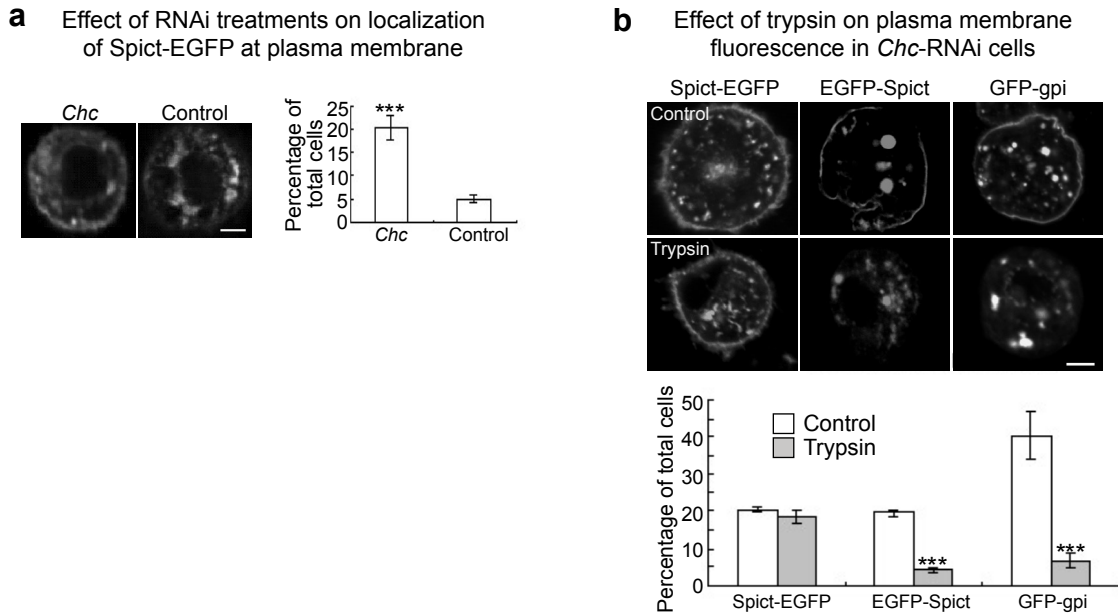


Supplementary Figure 1. Localization of tagged Spict.

(a) S2 cells expressing a Spict-EGFP fusion stained for other endosomal and lysosomal markers.

(b) Localization of Spict-mRFP (expressed using *Actin5C-GAL4* in a *spict^{mut}* background), Spinster, and LysoTracker staining, at muscles 6 and 7 of segment A2 of third instar larvae. The broken line shows the approximate boundary between muscles 6 and 7, along which the NMJ lies. All panels are single confocal sections. Scale bars: (a), 5 μm ; (b), 10 μm .

Supplementary Figure 2



Supplementary Figure 2. Topology of Spict in S2 cells.

This result is consistent with either of the previous suggestions that Spict family members might have nine transmembrane domains¹, or be divergent members of the 7-TM superfamily².

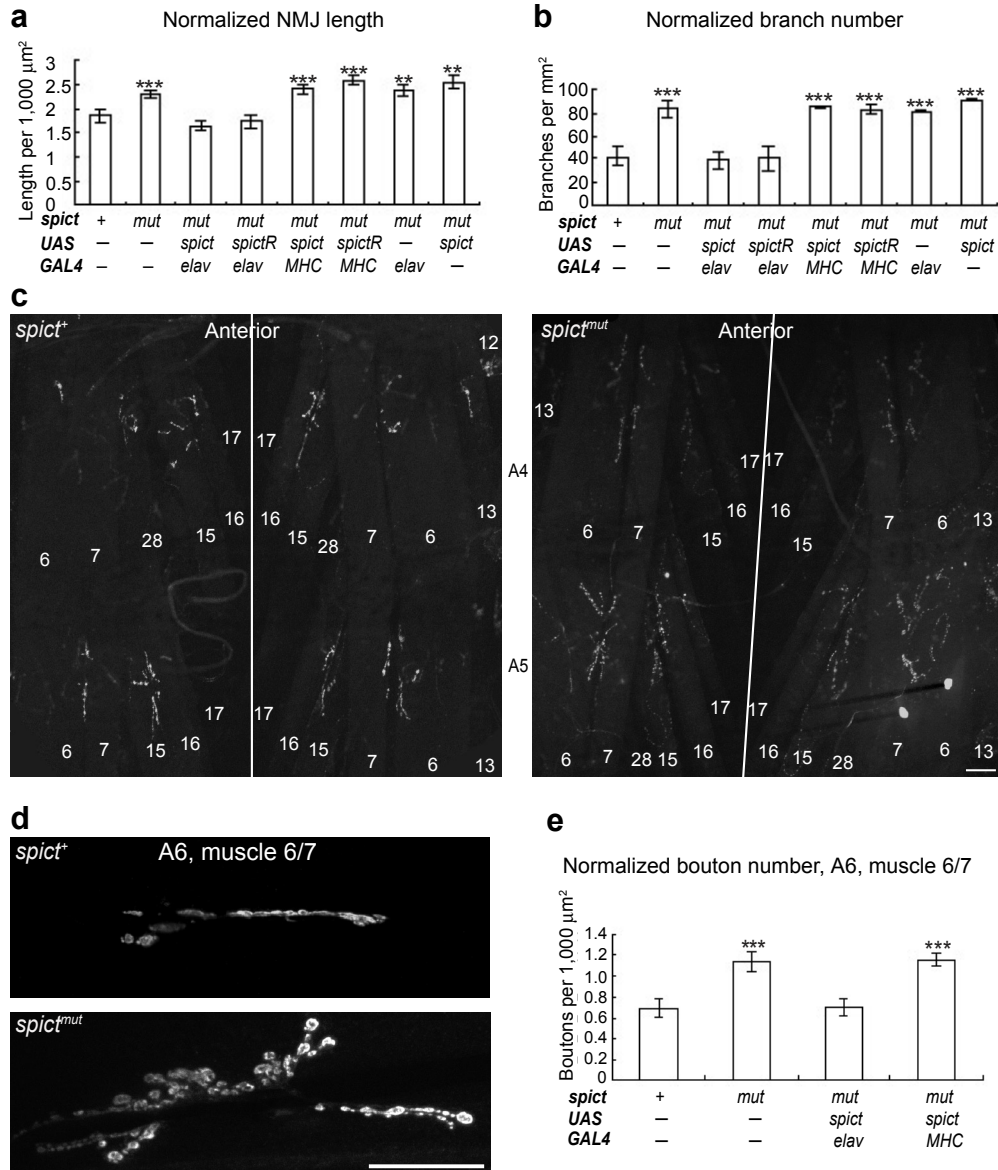
(a) We first tested whether Spict-EGFP or EGFP-Spict, expressed in S2 cells, could be redistributed to the plasma membrane by blockage of endocytosis. Treatment with RNAi against *clathrin heavy chain* (*Chc*) caused redistribution of the Spict fusions towards the plasma membrane. A Spict-EGFP expression vector was used to transfect S2 cells, along with different RNA molecules. Cells treated with double stranded *Chc* RNA, but not those treated with control RNA (*pTRI-Xef1*), redistributed Spict-EGFP to the plasma membrane. The left two panels show projections of confocal sections of typical cells; the right panel shows quantification of cells that had at least 30% of Spict-EGFP fluorescence within 0.5 μm of the cell surface. Scale bar, 5 μm .

(b) Fluorescence of EGFP-Spict, but not of Spict-EGFP, is susceptible to exogenously added trypsin. Double stranded *Chc* RNA, together with expression vectors for Spict-EGFP, EGFP-Spict or GFP-gpi, were used to transfect S2 cells, which were subsequently treated with trypsin. Trypsin treatment significantly reduced the number of cells with EGFP-Spict and GFP-gpi at the cell surface; in the case of Spict-EGFP, it had no significant effect ($P = 0.5$). This suggested that *clathrin* RNAi treatment redistributed the fusion proteins to the cell surface, and that the N-terminus of Spict is extracellular or luminal, and its C-terminus cytosolic. All panels show projections of confocal sections. For all comparisons with controls, *, $P < 0.05$; **, $P < 0.01$; ***, $P < 0.001$. $n=5$ transfections. Scale bars, 5 μm .

References

1. Chai, J.H., Locke, D.P., Greally, J.M., Knoll, J.H., Ohta, T., Dunai, J., Yavor, A., Eichler, E.E. & Nicholls, R.D. Identification of four highly conserved genes between breakpoint hotspots BP1 and BP2 of the Prader-Willi/Angelman Syndromes deletion region that have undergone evolutionary transposition mediated by flanking duplicons. *Am J Hum Genet.* **73**, 898-925 (2003).
2. Lefèvre, C., Bouadjar, B., Karaduman, A., Jobard, F., Saker, S., Ozguc, M., Lathrop, M., Prud'homme, J.F. & Fischer, J. Mutations in ichthyin a new gene on chromosome 5q33 in a new form of autosomal recessive congenital ichthyosis. *Hum. Mol. Gen.* **13**, 2473-2482 (2004).

Supplementary Figure 3



Supplementary Figure 3. *spict* null mutants cause synaptic overgrowth at the NMJ.

Quantification of normalized length (**a**) and branch numbers (**b**) of NMJs of muscle 6/7 of hemisegment A3, for each genotype shown in Fig. 3b. *spictR* represents *spict-mRFP*.

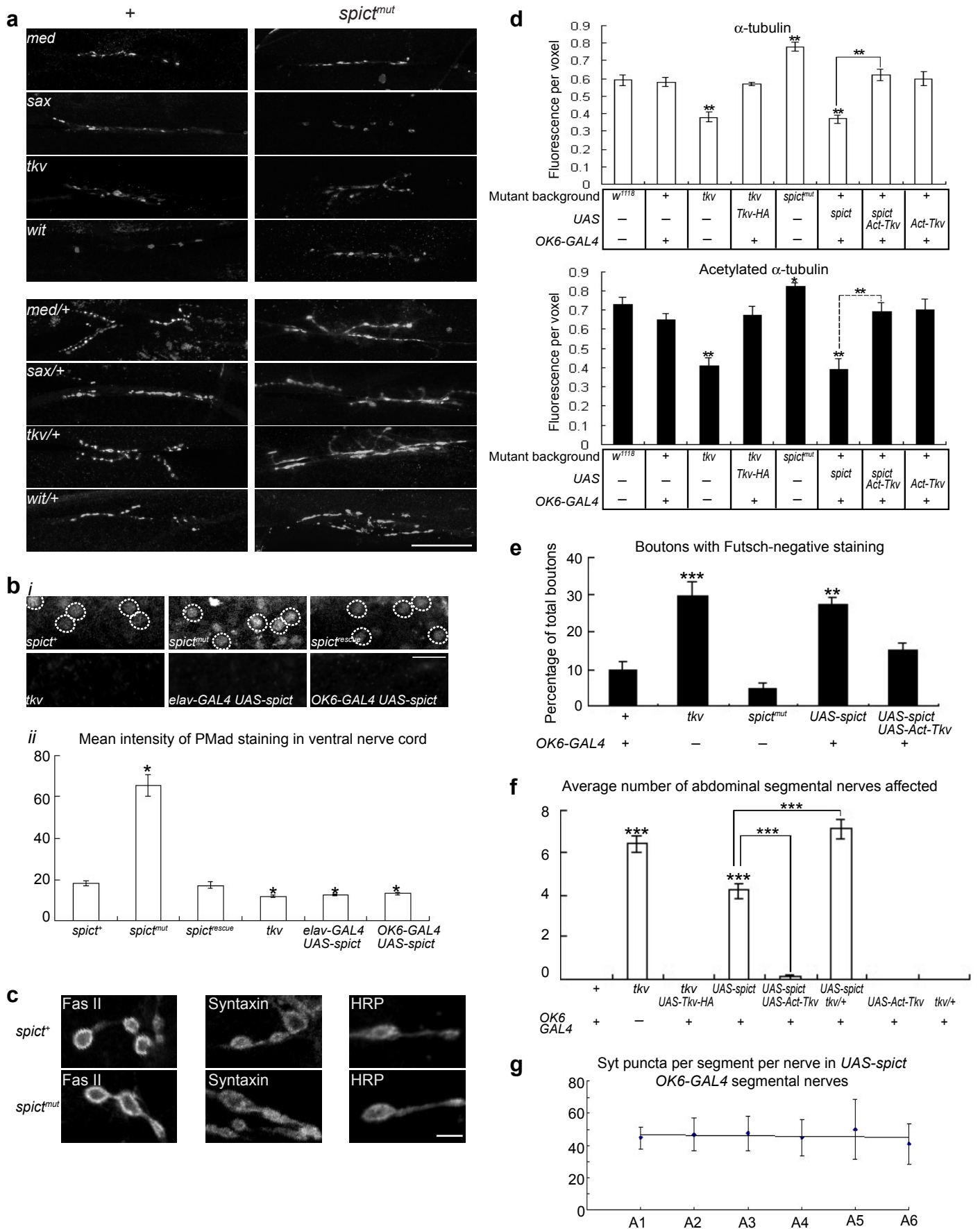
(**c**) NMJ overgrowth (shown by anti-synaptotagmin) in segments A4-5 in *spict^{mut}* third instar larvae. Anterior is on the top and midlines are indicated by near-vertical lines in the middle of each panel. Muscles are numbered. Synaptic boutons are stained by anti-synaptotagmin. Scale bar, 50 µm.

(**d**) NMJ overgrowth at muscle 6/7 of A6 in a *spict^{mut}* larva. Scale bar, 50 µm.

(**e**) Quantification of normalized bouton numbers in each genotype shown in **d** and in rescue genotypes.

Panels in **c** and **d** are projections of confocal sections. For comparisons with *spict*⁺: *, $P < 0.05$; **, $P < 0.01$; ***, $P < 0.001$. n=20 larvae.

Supplementary Figure 4



Supplementary Figure 5

